



Electronic multipoles and multiplet pairs induced by Pomeranchuk and Cooper instabilities of Bogoliubov Fermi surfaces

Shun-Ta Tamura, Shoma Iimura , and Shintaro Hoshino

Department of Physics, Saitama University, Shimo-Okubo, Saitama 338-8570, Japan

 (Received 15 April 2020; revised 31 May 2020; accepted 2 June 2020; published 6 July 2020)

It was recently pointed out that Fermi surfaces can remain even in superconductors under symmetric spin-orbit interaction and broken time-reversal symmetry. Using the linear response theory, we study the instability of such systems toward ordering, which is an intrinsic property of Fermi surfaces. The ordered states are classified into diagonal and off-diagonal ones, which respectively indicate the Pomeranchuk instability and Cooper pairing not of original electron but of Bogoliubov particles (bogolons). The corresponding order parameters are expanded by multipole moments (diagonal order parameter) and multiplet pair amplitudes (off-diagonal order parameter) of original electrons, which are induced by the internal fields arising from bogolon ordering. While the bogolons' order parameters partially inherit the characters of the original electrons, many order parameter components mix with similar magnitude. Hence, there is no clear-cut distinction for whether the phase transition is diagonal or off-diagonal ordering in terms of the original electrons. These ordering instabilities inside the superconducting states provide insights into superconductors which have the second phase transition below the first transition temperature.

DOI: [10.1103/PhysRevB.102.024505](https://doi.org/10.1103/PhysRevB.102.024505)

I. INTRODUCTION

Fermi surfaces are known to show a variety of intriguing phenomena at low temperatures because of the interaction effects among electrons. A typical example is the magnetic ordering, where the spin degrees of freedom near the Fermi energy are reconstructed by repulsive interactions. The critical value of the interaction where the order parameter, or magnetization, becomes finite is proportional to the inverse of the density of states known as the Stoner criterion. It has also been recognized that the presence of Fermi surfaces drives the system to nonmagnetic ordering, which results in spatial-symmetry lowering (Pomeranchuk instability [1]). The other examples where the Fermi surface effect is involved in mechanisms include the screening of the magnetic moments in metals known as the Kondo effect [2,3].

The superconducting state, which is caused by Cooper pair formation [4,5], is also a manifestation of the instability of Fermi surfaces, whose elementary fermionic excitations are described as emerging Bogoliubov quasiparticles (or bogolons) written in terms of the electron-hole superposed state [6]. The instability toward superconductivity is a quite general phenomenon, as evidenced by the logarithmically divergent pairing susceptibility at low temperatures even without interactions due to the presence of Fermi surfaces. Usually, the Fermi surfaces disappear in the resultant pairing state, and the system reaches the ground state with no more degrees of freedom left for electrons.

On the other hand, an interesting possibility was pointed out theoretically: the Bogoliubov particles can form stable Fermi surfaces in some superconductors (Bogoliubov Fermi

surfaces) [7–14]. It is also known that the degrees of freedom at the Fermi level in the superconducting state can also remain under a supercurrent flow [15–17]. As discussed above, the remaining Fermi surface has instabilities toward ordering, and here it appears *inside the superconducting state*. Because of the intrinsic logarithmically divergent pair susceptibility, it is naturally expected that the system with Bogoliubov Fermi surfaces shows a pairing state of bogolons at sufficiently low temperatures. Such a possibility was, indeed, studied recently [18]. In the present paper, we study the properties of both diagonal (Pomeranchuk instability) and off-diagonal (Cooper instability) order parameters of bogolons. In addition, in order to clarify their nature, we dissect the bogolons into the original electrons. Specifically, for the Cooper pairing of bogolons, since the pairing state of original electrons is already realized, the nature of the second pairing state inside the superconducting state is interesting but unclear. We discuss this “pairing state of the pairing state” based on a simple model that shows Bogoliubov Fermi surfaces. These insights can also provide a candidate scenario for the ordered states inside the superconducting state.

In this paper, using the $j = 3/2$ electron model [10,19–21] with Bogoliubov Fermi surfaces, we identify emergent order parameters of the original electrons that are induced by bogolons' diagonal and off-diagonal orderings. For this purpose, we employ the multipole expansion in terms of original electron degrees of freedom. The concept of electronic multipoles originated from the spin-orbital model [22] in d -electron systems and has been further extended to f -electron and other systems [23–33]. Since the pairing amplitudes are also involved in the superconducting state, we need to extend the multipole expansion to include pair amplitudes on

equal footing. As a result, the bogolon order parameters are represented by a mixture of diagonal and off-diagonal order parameters of original electrons. Hence, while the ordering of bogolons is a good physical picture, we cannot simply classify them as either diagonal or off-diagonal orders of the original electrons.

This paper is organized as follows. In the next section we show the formulations for the Bogoliubov Fermi surface and the order parameters. The numerical results are given in Sec. III. We summarize the paper in Sec. IV and make a comment on the relevance to real materials. Full lists of multipole operators, multiplet pair amplitudes, and form factors in the wave vector space are given in Appendixes A and B.

II. FORMULATION

A. Model Hamiltonian

We take the simplest model that has stable Bogoliubov Fermi surfaces as introduced in Ref. [10]. We consider the continuum model by focusing on a part of the Brillouin zone. The Hamiltonian reads

$$\mathcal{H} = \sum_{\mathbf{k}} \bar{c}_{\mathbf{k}}^{\dagger} [\alpha(\mathbf{k}^2 - k_F^2) \hat{1} + \beta(\mathbf{k} \cdot \hat{\mathbf{J}})^2] \bar{c}_{\mathbf{k}} + \sum_{\mathbf{k}} (\bar{c}_{\mathbf{k}}^{\dagger} \hat{\Delta}_{\mathbf{k}} \bar{c}_{-\mathbf{k}}^{\dagger} + \text{H.c.}), \quad (1)$$

where $\bar{c}_{\mathbf{k}} = (c_{\mathbf{k}, \frac{3}{2}}, c_{\mathbf{k}, \frac{1}{2}}, c_{\mathbf{k}, -\frac{1}{2}}, c_{\mathbf{k}, -\frac{3}{2}})^T$ is the spin-3/2 spinor composed of electron annihilation operators. The hat ($\hat{\cdot}$) symbol represents a 4×4 matrix. $\hat{\mathbf{J}}$ is the angular momentum matrix for $j = 3/2$ [see Eqs. (A3)–(A5)]. The parameter α is a constant proportional to the inverse of mass, k_F is the Fermi wave vector, and β is the symmetric spin-orbit coupling. The Fermi energy is given by $\varepsilon_F = \alpha k_F^2$. The gap parameter is chosen as

$$\hat{\Delta}_{\mathbf{k}} = \Delta_1 k_z (k_x + ik_y) \hat{E} + \frac{2}{\sqrt{3}} \Delta_0 [\hat{J}_z (\hat{J}_x + i\hat{J}_y)] \hat{E}, \quad (2)$$

where the brackets $[\dots]$ symmetrize the expression as $[AB] = (AB + BA)/2$. We have defined the antisymmetric tensor \hat{E} [see Eq. (A18)]. The above Hamiltonian guarantees the presence of the stable Fermi surfaces even in the superconducting state with $\Delta_{0,1} \neq 0$ [10]. Hence, we naively expect another phase transition at low enough temperatures. Once the Hamiltonian is fixed in this way, we can move to a diagonalized picture as

$$\mathcal{H} = \sum_{\mathbf{k} \in \text{HBZ}} \bar{\psi}_{\mathbf{k}}^{\dagger} \check{H}_{\mathbf{k}} \bar{\psi}_{\mathbf{k}} = \sum_{\mathbf{k} \in \text{HBZ}} \bar{\alpha}_{\mathbf{k}}^{\dagger} \check{\Lambda}_{\mathbf{k}} \bar{\alpha}_{\mathbf{k}}, \quad (3)$$

where $\bar{\psi}_{\mathbf{k}} = (\bar{c}_{\mathbf{k}}^{\dagger}, \bar{c}_{-\mathbf{k}}^{\dagger})^T$ is the eight-component Nambu spinor and $\bar{\alpha}_{\mathbf{k}} = \check{U}_{\mathbf{k}}^{\dagger} \bar{\psi}_{\mathbf{k}}$ is the Bogoliubov particle annihilation operators with a diagonal eigenvalue matrix $\check{\Lambda}_{\mathbf{k}}$ and eigenvector matrix $\check{U}_{\mathbf{k}}$. The check ($\check{\cdot}$) symbol represents an 8×8 matrix. Note that the wave vector summation is taken over the half Brillouin zone (HBZ) to avoid double counting.

Since the low-temperature behaviors are dominated by the degrees of freedom near the Fermi level, we can construct the effective low-energy model involving only the HBZ. There are doubly degenerate components near the Fermi level protected by the particle-hole symmetry, which are labeled 1 and 2, and

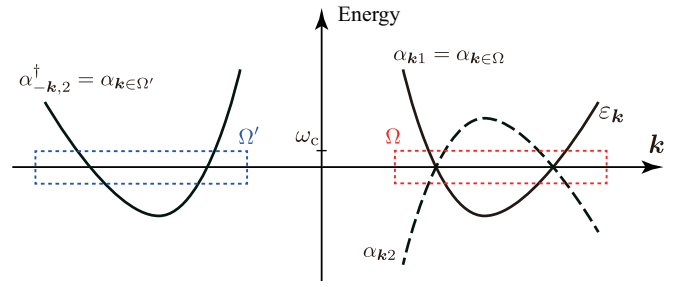


FIG. 1. Illustration of the band structures of bogolons near the Fermi level. The regions enclosed by dotted lines show the low-energy windows relevant to instability of Bogoliubov Fermi surfaces.

the corresponding effective low-energy Hamiltonian is written as

$$\mathcal{H}_{\text{eff}} = \sum_{\mathbf{k} \in \Omega} (\varepsilon_{k1} \alpha_{k1}^{\dagger} \alpha_{k1} + \varepsilon_{k2} \alpha_{k2}^{\dagger} \alpha_{k2}), \quad (4)$$

where $\varepsilon_{k1} = -\varepsilon_{k2} \equiv \varepsilon_{\mathbf{k}}$. The region Ω represents a wave vector space near the Fermi surfaces. Whereas the energy is dependent on the pseudospin index (1, 2), it is more convenient to define another spinless fermion $\alpha_{\mathbf{k} \in \Omega} = \alpha_{k1}$ and $\alpha_{\mathbf{k} \in \Omega'} = \alpha_{-k,2}^{\dagger}$ (see Fig. 1 for schematic pictures of band structures and the definition of Ω'). Then we obtain the simple spinless Hamiltonian

$$\mathcal{H}_{\text{eff}} = \sum_{\mathbf{k} \in \Omega + \Omega'} \varepsilon_{\mathbf{k}} \alpha_{\mathbf{k}}^{\dagger} \alpha_{\mathbf{k}}, \quad (5)$$

where the constant term is dropped. We have used the relation $\varepsilon_{-\mathbf{k}} = \varepsilon_{\mathbf{k}}$. Since one sees the unclosed Fermi surfaces for $\mathbf{k} \in \text{HBZ}$ in Eq. (4), the Hamiltonian (5) is a more natural representation where only closed Fermi surfaces exist. We have inversion symmetry in Eq. (5), which is seen as the particle-hole symmetry in terms of Eq. (4).

B. Order parameter and susceptibility

With the Hamiltonian (5), the analogy to spinless fermions can be used, and now we are ready to define the possible order parameters of bogolons. We have two kinds of order parameters, i.e., diagonal (Pomeranchuk instability) and off-diagonal (Cooper instability) ones. The former is defined by

$$\mathcal{N}_{D,\eta} = \sum_{\mathbf{k} \in \Omega + \Omega'} g_{\eta}(\mathbf{k}) \alpha_{\mathbf{k}}^{\dagger} \alpha_{\mathbf{k}}, \quad (6)$$

where the symbol D represents a diagonal component. η represents polynomials such as $g_{\eta=\text{xy}}(\mathbf{k}) \propto k_x k_y$ (see Appendix B for more details), which determines the spatial structure. In principle, one can also consider the combination of these types, for example, $g_{\eta}(\mathbf{k}) \propto k_x + ik_y$. The instability toward these orders can be studied based on the susceptibility defined by

$$\chi_{D,\eta} = \int_0^{1/T} d\tau \langle \mathcal{N}_{D,\eta}(\tau) \mathcal{N}_{D,\eta}^{\dagger} \rangle. \quad (7)$$

The Heisenberg picture with imaginary time is defined as $\mathcal{O}(\tau) = e^{\tau \mathcal{H}_{\text{eff}}} \mathcal{O} e^{-\tau \mathcal{H}_{\text{eff}}}$, and the brackets $\langle \dots \rangle$ indicate the quantum statistical average using \mathcal{H}_{eff} . The physical meaning

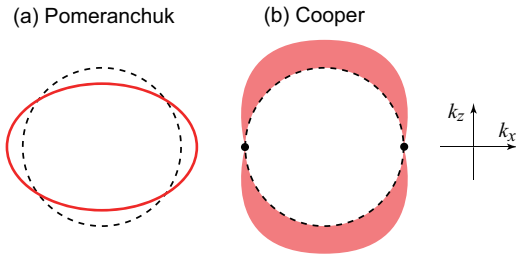


FIG. 2. Schematic pictures for (a) diagonal and (b) off-diagonal orders of the $\eta = z$ type [$g_z(\mathbf{k}) \propto k_z$]. The dashed line shows the bare Fermi surface without ordering. The solid line in (a) shows the deformed Fermi surface due to the Pomeranchuk instability. The shaded area in (b) shows the magnitude of the gap induced by the Cooper instability.

of this quantity is how much of the order parameter is induced as $\langle \mathcal{N}_{D,\eta} \rangle = \chi_{D,\eta} h_{D,\eta}$ under the test field $h_{D,\eta}$ conjugate to $\mathcal{N}_{D,\eta}$. The schematic picture of Pomeranchuk instability is shown in Fig. 2(a). As shown later, this is simply evaluated to give $\chi_{D,\eta} \sim \rho$, with ρ being a density of states at the Fermi level.

If the interaction term $\mathcal{H}_{\text{int}} = -U \mathcal{N}_{D,\eta}^2$ with $U > 0$ is present in the Hamiltonian, this susceptibility is enhanced by the factor $(1 - U \chi_{D,\eta})^{-1}$ according to the random-phase approximation justified in the weak-coupling limit. Hence, the ordering occurs when the Stoner condition $\rho U \gtrsim 1$ is satisfied. On the other hand, it is hard to tell which type of interaction is most relevant since it is dependent on the form of the interactions among the original electrons, which are, in general, dressed by the phonons and spin and/or orbital fluctuations. Hence, below we assume the existence of the one relevant interaction which favors the appearance of the order parameter $\langle \mathcal{N}_{D,\eta} \rangle$.

At this point, we introduce the matrix $\hat{O}^{\eta'}$ related to the multipoles, where η' again represents polynomial functions. The full functional forms are given in Appendix A and are classified into one monopole ($\hat{O}^1 \sim \hat{1}$ with the identity $\hat{1}$), three dipoles (e.g., $\hat{O}^x = \hat{J}^x$), five quadrupoles (e.g., $\hat{O}^{xy} \sim \hat{J}^x \hat{J}^y$), and seven octupoles (e.g., $\hat{O}^{xyz} \sim \hat{J}^x \hat{J}^y \hat{J}^z$). These are called electronic multipoles in this paper. With the above 16 matrices, any 4×4 matrix can be expanded. For example, the spin-orbit interaction term with β [Eq. (1)] is expressed by the quadrupoles. We can also classify the pairing amplitudes by the matrix $\hat{O}^{\eta'} \hat{E}$ as spin singlet ($\eta' = 1$), spin triplet (e.g., $\hat{O}^x \hat{E}$), spin quintet (e.g., $\hat{O}^{xy} \hat{E}$), and spin septet (e.g., $\hat{O}^{xyz} \hat{E}$), which are called electronic multiplet pairs. Our choice of the pair potential in Eq. (2) is regarded as a mixture of the spin singlet and spin quintet [10].

It is interesting to see the bogolons' physical quantities in terms of the *original electrons*. The operator for the bogolons' order parameter is expanded by the multipole operators of electrons as

$$\begin{aligned} \mathcal{N}_{D,\eta} &= \sum_{\mathbf{k} \in \Omega} \sum_{\eta'} \sum_{\xi' = D, \bar{D}, \bar{O}, \bar{O}} C_{D,\eta}^{\xi'\eta'}(\mathbf{k}) \bar{\psi}_{\mathbf{k}}^\dagger \hat{O}^{\xi'\eta'} \bar{\psi}_{\mathbf{k}} + \text{const} \quad (8) \\ &\equiv \sum_{\xi'\eta'} \mathcal{M}_{D,\eta}^{\xi'\eta'} + \text{const}. \quad (9) \end{aligned}$$

The 8×8 matrix $\hat{O}^{\xi'\eta'}$ composed of $\hat{O}^{\eta'}$ and \hat{E} specifies the type of electron multipole defined in Appendix A 3. Equation (9) shows that the operator $\mathcal{N}_{D,\eta}$ for bogolons includes the diagonal component $\mathcal{M}^{\xi' = D, \bar{D}}$, where D and \bar{D} represent even-parity and odd-parity multipoles. These two types ($\xi' = D, \bar{D}$) can be constructed due to the enlargement of the single-particle Hilbert space involving the \mathbf{k} and $-\mathbf{k}$ components. Note that the internal $j = 3/2$ degrees of freedom are regarded as independent from the parity here (\mathbf{k} parity). We also have the off-diagonal components $\mathcal{M}^{\xi' = O, \bar{O}}$ of the original electrons due to the gauge symmetry breaking by $\hat{\Delta}_{\mathbf{k}}$, where the symbol O shows an electron pair ($c^\dagger c^\dagger$ type) and \bar{O} shows a hole pair (cc type). The expansion coefficient C in Eq. (9) will be evaluated in the next section.

The above discussion is also extended to the pairing state of bogolons [18]:

$$\mathcal{N}_{O,\eta} = \sum_{\mathbf{k} \in \Omega + \Omega'} g_\eta(\mathbf{k}) \alpha_{\mathbf{k}}^\dagger \alpha_{-\mathbf{k}}^\dagger, \quad (10)$$

where the symbol O in the left-hand side represents an off-diagonal component (Cooper pairing). Since the present Bogoliubov Fermi surfaces do not have internal degrees of freedom, the form factor must satisfy $g_\eta(-\mathbf{k}) = -g_\eta(\mathbf{k})$ (odd parity) due to the Pauli principle. The multipole expansion is performed as

$$\mathcal{N}_{O,\eta} = \sum_{\mathbf{k} \in \Omega} \sum_{\xi'\eta'} C_{O,\eta}^{\xi'\eta'}(\mathbf{k}) \bar{\psi}_{\mathbf{k}}^\dagger \hat{O}^{\xi'\eta'} \bar{\psi}_{\mathbf{k}} \quad (11)$$

$$\equiv \sum_{\xi'\eta'} \mathcal{M}_{O,\eta}^{\xi'\eta'}. \quad (12)$$

The noninteracting pair susceptibility $\chi_{O,\eta}$, which is defined in a manner similar to Eq. (7), is evaluated to give $\chi_{O,\eta} \sim \rho \ln(\omega_c/T)$, with ω_c being a cutoff energy. When the attractive interaction $\mathcal{H}_{\text{int}} = U \mathcal{N}_{O,\eta} \mathcal{N}_{O,\eta}^\dagger$ with $U < 0$ exists, the pairing susceptibility is enhanced by the factor $(1 + U \chi_{O,\eta})^{-1}$, and the logarithmic divergence gives rise to the pairing state below the finite transition temperature $T_c \sim \omega_c \exp(-\frac{1}{\rho|U|})$. The schematic picture of the Cooper instability is shown in Fig. 2(b).

Summing up the above expressions, we can rewrite the linear response formula $\langle \mathcal{N}_{\xi\eta} \rangle = \chi_{\xi\eta} h_{\xi\eta}$ as

$$\langle \mathcal{M}_{\xi\eta}^{\xi'\eta'} \rangle = \chi_{\xi\eta}^{\xi'\eta'} h_{\xi\eta}, \quad (13)$$

$$\chi_{\xi\eta}^{\xi'\eta'} = \int_0^{1/T} d\tau \langle \mathcal{M}_{\xi\eta}^{\xi'\eta'}(\tau) \mathcal{N}_{\xi\eta}^\dagger \rangle, \quad (14)$$

with the sum rule

$$\chi_{\xi\eta} = \sum_{\xi'\eta'} \chi_{\xi\eta}^{\xi'\eta'}. \quad (15)$$

The physical meaning of $\chi_{\xi\eta}^{\xi'\eta'}$ in Eq. (13) is as follows: once the internal test field $h_{\xi\eta}$ corresponds to the diagonal ($\xi = D$) or off-diagonal ($\xi = O$) ordering of bogolons, the conjugate order parameter $\langle \mathcal{N}_{\xi\eta} \rangle$ of bogolons is induced simultaneously, which is composed of the multipoles ($\xi' = D, \bar{D}$) and multiplet pairs ($\xi' = O, \bar{O}$) of original electrons of type η' (see Table I). Simply speaking, the susceptibility gives information on what types of electron multipoles or Cooper pairs are

where the energy-dependent function is given by

$$P_{\xi=D}(\varepsilon) = -\frac{\partial f(\varepsilon)}{\partial \varepsilon}, \quad (24)$$

$$P_{\xi=0}(\varepsilon) = -\frac{f(\varepsilon) - f(-\varepsilon)}{2\varepsilon}. \quad (25)$$

We have introduced the Fermi distribution function $f(\varepsilon) = 1/(e^{\varepsilon/T} + 1)$.

Now we perform the \mathbf{k} integral. Since our system has rotational symmetry around the z axis, the cylindrical coordinate $\mathbf{k} = (k, \phi, k_z)$ with $k_x = k \cos \phi$ and $k_y = k \sin \phi$ is convenient. The unitary matrix that diagonalizes the original Hamiltonian is transformed by the rotation along the k_z axis as

$$\check{U}_{\mathbf{k}} = \check{U}(k, \phi, k_z) = \check{R}(\phi)\check{U}(k, 0, k_z), \quad (26)$$

$$\check{R}(\phi) = \begin{pmatrix} \exp[-i(\hat{J}_z - \frac{1}{2}\hat{1})\phi] & \hat{0} \\ \hat{0} & \exp[i(\hat{J}_z - \frac{1}{2}\hat{1})\phi] \end{pmatrix}. \quad (27)$$

The matrix \check{R} represents a rotation around the k_z axis, which connects different \mathbf{k} points in the xy plane. Since the form factor g_η is written as $g_\eta(\mathbf{k}) = g'_\eta(k, k_z)f_\eta(\phi)$ (see Appendix B for its concrete form), the ϕ integral in evaluating the susceptibility can be performed analytically, and the other integrals are considered within the k_x - k_z plane. It is also convenient to change the coordinate system as $(k, k_z) \rightarrow (k_\perp, k_\parallel)$, which is the \mathbf{k} coordinates normal and parallel to the Fermi surface. The coordinate k_\perp can be changed into the energy integral as $d\varepsilon = vdk_\perp$, where v is the Fermi velocity. After some calculations, one reaches the expression

$$\begin{aligned} \chi_{\xi\eta}^{\xi'\eta'} &\simeq \frac{1}{(2\pi)^2} \int_{-\omega_c}^{\omega_c} d\varepsilon P_\xi(\varepsilon) \int_{k_x, k_z > 0} dk_\parallel \frac{k_x(k_\parallel) |g'_\eta(k_\parallel)|^2}{|v(k_\parallel)|} \\ &\times \sum_{ijkl} O_{ij}^{\xi'\eta'} [\check{U}(k_\parallel) \check{n}_{\xi\eta} \check{U}^\dagger(k_\parallel)]_{ji} \Gamma_{ijkl}^\eta \\ &\times O_{kl}^{\xi'\eta'} [\check{U}(k_\parallel) \check{n}_{\xi\eta} \check{U}^\dagger(k_\parallel)]_{lk}, \end{aligned} \quad (28)$$

where we have introduced the cutoff energy ω_c and have simplified the expression by assuming that the dominant contribution comes from the Fermi surface, i.e., $\varepsilon = 0$. This expression is based on the energy separation $\varepsilon_{\text{BF}} \gg \omega_c \gg T$ as in the standard BCS theory, where ε_{BF} is the Fermi energy for the Bogoliubov Fermi surface. The ϕ -integral part is separately given as

$$\Gamma_{ijkl}^\eta = \int \frac{d\phi}{2\pi} |f_\eta(\phi)|^2 e^{i(n_i - n_j + n_k - n_l)\phi}, \quad (29)$$

where the integer n_i is defined by $R_{ii}(\phi) = e^{-in_i\phi}$. The function Γ_{ijkl}^η can be evaluated by using the information in Appendix B. Thus, we have to evaluate only the k_\parallel line integral along the Fermi surface, which is performed numerically with the discretized mesh. Since the wave vector \mathbf{k} belongs to Ω , the k_\parallel integral is performed within the region of $k_x, k_z > 0$.

D. Interpretation in terms of Landau theory

Before showing the numerical results, let us discuss the Landau free energy relevant to Pomeranchuk and Cooper instabilities of bogolons to understand the induced electron

multipoles and multiplet pairs. We consider one of the bogolon orderings whose order parameter is denoted as n ($=\langle \mathcal{N}_{\xi\eta} \rangle$), where we have omitted the index (ξ, η) for simplicity. The corresponding physical quantities for original electrons are written as m_i ($\sim \langle \mathcal{M}_{\xi\eta}^{\xi'\eta'} \rangle$), where we have used the short-hand notation $i = (\xi'\eta')$. Since some of the electron multipoles are finite from the beginning in our model, m_i is defined as a deviation from its equilibrium point. The Landau free energy is explicitly written down as

$$F = an^2 + bn^4 - h_{\text{ext}}n + \sum_i g_i n m_i + \sum_i a'_i m_i^2. \quad (30)$$

Here h_{ext} is an imaginary test field for bogolons, and g_i is the coupling between the bogolons' and electrons' order parameters. We assume $a'_i > 0$ and $b > 0$, which guarantees the thermodynamic stability.

The first term on the right-hand side represents a distance to the critical point and is rewritten as

$$an^2 = a_0 n^2 - h_{\text{MF}}(n)n, \quad (31)$$

where $a_0^{-1} (>0)$ is a free susceptibility without interactions and $h_{\text{MF}} = In$ is the internal mean field induced by an effective interaction I . In order to have intuition for Eq. (31), let us consider the two examples. First, if the noninteracting susceptibility shows Curie law as $a_0(T)^{-1} \sim \frac{1}{T}$, we have in the presence of interaction the Curie-Weiss law $a(T)^{-1} \sim \frac{1}{T - T_c}$, with the Curie temperature $T_c \sim I$ determined by the condition $a = 0$. Second, if we consider a pairing state of electrons, we have $a_0(T)^{-1} \sim \rho \ln \frac{\omega_c}{T}$ from the Fermi surface instability. Then the full inverse susceptibility is given by $a(T) \sim \rho I^2 \ln \frac{T}{T_c}$, with the superconducting transition temperature $T_c \sim \omega_c \exp(-\frac{1}{\rho I})$, which corresponds to a standard result of the BCS theory. We note that, as seen below, the transition temperature is modified once the order parameter n couples to the other ones (m_i) linearly.

Above the transition temperature of the bogolon ordering, the order parameters n, m_i are just induced by the external field. The resultant order parameters are given by

$$n = \chi h_{\text{ext}}, \quad (32)$$

$$m_i = f_i n = f_i \chi h_{\text{ext}}, \quad (33)$$

where the susceptibility χ and the factor f_i are

$$\chi = \left(2a - \sum_i 2a'_i f_i^2 \right)^{-1}, \quad (34)$$

$$f_i = -\frac{g_i}{2a'_i}. \quad (35)$$

According to Eq. (15), there is the sum rule $n = \sum_i m_i$, or

$$\sum_i f_i = 1. \quad (36)$$

Thus, the magnitude of the electron order parameter induced by external field for bogolons is controlled by the factor f_i . What we have calculated in Eq. (28) is equivalent to the quantity f_i . Although the interactions in general modify the coefficients, we have assumed the weak-coupling limit, and the corrections are regarded as irrelevant for a'_i, g_i , and b in the

leading-order contribution. We remark that near the transition temperature the interaction effect is relevant for the coefficient a even in the weak-coupling limit, but the quantity f_i (as will be shown in Sec. III B) is not dependent on a .

If one traces out m_i from the equations of state, only the order parameter n enters the Landau theory, and the coefficient a is replaced by $\chi^{-1}/2$. The n -only model corresponds to the effective low-energy model in Eq. (5), which does not include the information for the original electrons.

Below the transition temperature determined by $\chi^{-1} = 0$, on the other hand, the bogolon order parameter and corresponding electron order parameters are induced by the self-consistent internal field as

$$n = \frac{1}{I} h_{\text{MF}}, \quad (37)$$

$$m_i = f_i n = \frac{f_i}{I} h_{\text{MF}}, \quad (38)$$

where $1/I$ plays the role of susceptibility for the internal mean field. Note that the factor f_i is the same as the one above the transition temperature. Hence, if we would like to know the electrons' multipole components in the bogolons' ordered state, we have to calculate only the factor f_i in the bogolons' disordered phase. In the next section, we show the numerical results for f_i calculated in the presence of Bogoliubov Fermi surfaces.

III. NUMERICAL RESULTS

A. Bogoliubov Fermi surfaces

Before showing the susceptibilities, let us first discuss the Bogoliubov Fermi surfaces in our setup. Figures 3(a) and 3(b) show the shapes of Fermi surfaces in the presence of the pair potential, where the parameters are chosen to be $\beta = 0.1$, $\Delta_0 = 0.1$, $\Delta_1 = 0.5$ with the energy unit $\varepsilon_F = \alpha k_F^2 = 1$. In this case we have two Fermi surfaces in the first quadrant of the k_x - k_z plane, which are separately shown in Figs. 3(a) and 3(b). Depending on the choice of parameters, the number of Fermi surfaces changes, and we can have four Fermi surfaces in total, as shown in Figs. 3(c) and 3(d) for the parameters $\beta = 0.3$, $\Delta_0 = 0.1$, $\Delta_1 = 0.5$. In fact, the shapes of the Fermi surfaces in Figs. 3(a) and 3(b) [and also Figs. 3(c) and 3(d)] are the same if they are inverted at the $k_z = k_x$ line since the eigenenergies of $\hat{H}(k_x, 0, k_z)$ are identical to those of $\hat{H}(k_z, 0, k_x)$.

For comparison, the normal-state Fermi surfaces without pair potentials are also drawn with yellow lines. We can see from Figs. 3(a) and 3(b) that the Fermi surfaces near the k_z and k_x axes are not much modified, and away from the axes the deviation becomes larger. The wave function on the Fermi surface also remains unchanged near the axes, i.e., no mixture of electrons and holes, which is related to the disappearance of the pair potential proportional to Δ_1 in Δ_k .

The green-shaded area enclosed by the Fermi surface is related to the three-dimensional Fermi volume if one rotates the plane around the k_z axis. Then the Fermi volume near the k_z axis is pancakelike, and the one near the k_x axis is donutlike [10]. The Fermi surfaces around the k_x axis in Figs. 3(b) and 3(d) are away from the k_z axis, and the volume is much larger than the ones around the k_z axis. The Fermi volume near the

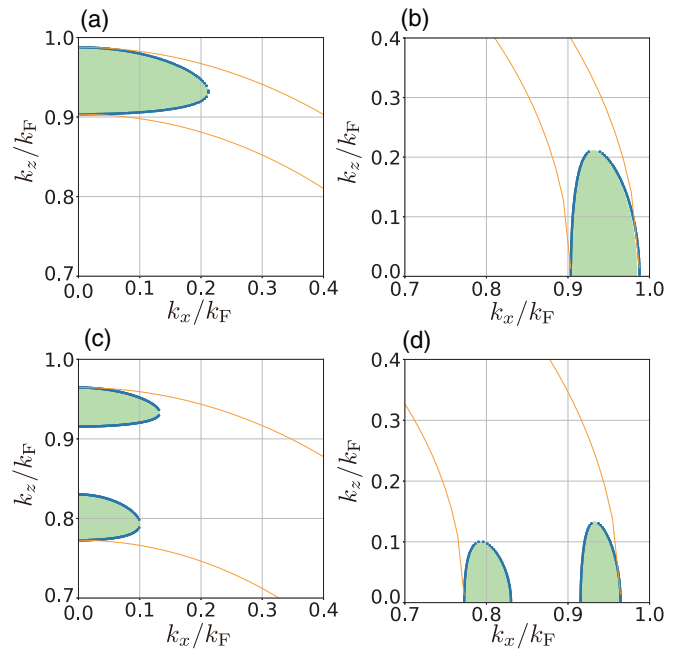


FIG. 3. Shapes of Bogoliubov Fermi surfaces. The parameters are chosen as $\beta/\varepsilon_F = 0.1$, $\Delta_0/\varepsilon_F = 0.1$, $\Delta_1/\varepsilon_F = 0.5$ for (a) and (b) and $\beta/\varepsilon_F = 0.3$, $\Delta_0/\varepsilon_F = 0.1$, $\Delta_1/\varepsilon_F = 0.5$ for (c) and (d). The electron Fermi surfaces without pair potentials are drawn by yellow solid lines. The blue dots show the Bogoliubov Fermi surface with the enclosed Fermi volume shaded in green.

k_z axis is roughly ten times smaller than the one near the k_x axis. Although the larger Fermi volume induces the larger instability toward ordering, which Fermi surface dominantly contributes depends on the form factor $g_\eta(\mathbf{k})$.

We comment on another system that exhibits Bogoliubov Fermi surfaces. The Bogoliubov Fermi surfaces inside the superconducting states are also proposed in the context of the Kondo lattice, which is one of the basic models for heavy-electron materials [36–40]. Here the origin of the peculiar superconductivity is the nontrivial effective hybridization between conduction and localized electrons, and the time-reversal symmetry breaking is not necessary for the mechanism. These systems should also show further ordering instabilities similar to those discussed in our paper.

B. Susceptibility tensors

According to the results in the last section, the noninteracting susceptibility can be written as

$$\chi_{\xi\eta}^{\xi'\eta'}(T) = \tilde{\chi}_{\xi\eta}^{\xi'\eta'} Q_\xi(T), \quad (39)$$

where $Q_D(T) = 1$ and $Q_O(T) = \ln(2e^\gamma \omega_c / \pi T)$, with the Euler's constant $\gamma \simeq 0.577$. Since the temperature-dependent part is not affected by the choice of η, η' , we have to numerically evaluate only the temperature-independent coefficient $\tilde{\chi}_{\xi\eta}^{\xi'\eta'} (> 0)$. The overall tendency of these physical quantities is not sensitive to the choice of the parameters. Hence, below we concentrate on the results for the parameters $\beta = 0.1$, $\Delta_0 = 0.1$, $\Delta_1 = 0.5$, whose Fermi surfaces are shown in Figs. 3(a) and 3(b). The information on Fermi surfaces is

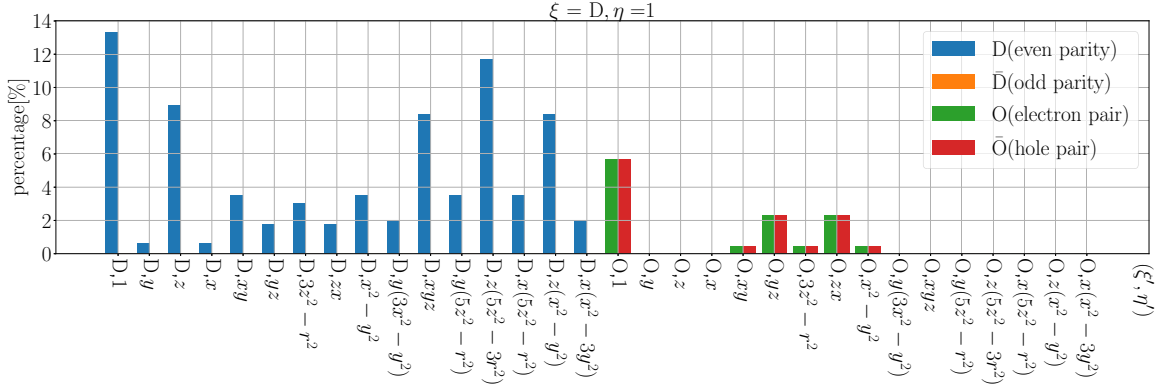


FIG. 4. Electron multipole components $\chi_{D,1}^{\xi'\eta'}$ induced by the increased chemical potential for bogolons which form the Fermi surfaces. The sum of the heights of bars is normalized to 100%. The parameters are chosen to be $\beta/\varepsilon_F = 0.1$, $\Delta_0/\varepsilon_F = 0.1$, $\Delta_1/\varepsilon_F = 0.5$.

extracted by dividing the k_x - k_z plane around the Fermi surface with 100×400 grids and by using the linear interpolation. We have checked that, quantitatively, the same results are obtained for the finer mesh.

Figure 4 shows the normalized susceptibility coefficient $\tilde{\chi}_{\xi\eta}^{\xi'\eta'}$ defined in Eq. (39). Here $\xi = D$ and $\eta = 1$ (s wave) are chosen for the bogolon component, and the values are normalized by the constant $C_{\xi\eta} = \sum_{\xi'\eta'} \tilde{\chi}_{\xi\eta}^{\xi'\eta'}$ to be 100% in total. This ($\xi = D, \eta = 1$) component indicates the deviation induced by the symmetric chemical potential field for bogolons, which does not break the symmetry of the original Hamiltonian in Eq. (5). Hence, the finite values in Fig. 4 indicate the components that are originally finite without Pomeranchuk or Cooper instabilities. Note that some components (e.g., $\eta' = x$ and $\eta' = y$) have the same value due to the symmetry.

One may have the impression that the finite $\eta' = x$ component ($\sim \hat{J}_x$) breaks the rotational symmetry around the z axis and is not consistent with the disordered situation. This discrepancy, at first sight, is rationalized by noticing the fact that the multipole component in Fig. 4 concerns the internal degrees of freedom of the $j = 3/2$ electron. The quantity is evaluated by the \mathbf{k} integral in Eq. (23), and the \mathbf{k} dependence does not explicitly appear. Hence, if one considers the multipole expansions in \mathbf{k} space, the combination of (k_x, k_y, k_z) and \hat{J}_x can lead to a scalar component which does not break the original symmetry. One can also show that the $\eta' = x$ component, which is absent in the original Hamiltonian, is induced in the Green's function in Eq. (22), which is more directly connected to the physical quantities. On the other hand, the odd-parity component and the spin-triplet and -septet pair amplitudes cannot appear with a scalar form. Then one needs spontaneous symmetry breaking by either the Pomeranchuk or Cooper instability.

Next, we discuss the results for symmetry-broken states of bogolons. Since the results for p -wave ordering are similar to those for f -wave ordering, here we focus on the case with $\eta = z, x$. Although we can also consider the d -wave components for the Pomeranchuk instability as in Table I(a), the results are similar to the s -wave case in Fig. 4. This is because the \mathbf{k} dependences do not explicitly enter in our multipole expansion, as discussed above. For the type of $\eta = xy$, for example, we have the $k_x k_y$ -type order parameter

within the charge sector ($\xi' = D, \eta' = 1$), which is zero in the disordered phase but finite below T_c . However, this type of order parameter cannot be explicitly seen in plots such as in Fig. 4, where one sees only the \mathbf{k} -summed multipole expansion coefficients with respect to the internal degrees of freedom of $j = 3/2$ electrons. In order to look at the symmetry breakings of d -wave type, spectral decomposition in terms of the angle ϕ functions is necessary. Moreover, for a material-specific case, the Fermi surfaces are, in general, anisotropic, and classification based on irreducible representations is necessary [11]. This decomposition is, in principle, possible, but here we focus on the typical cases of p -wave types to demonstrate the concept of the bogolon orderings and their interpretation in terms of $j = 3/2$ internal degrees of freedom of original electrons.

Figure 5 shows the results for the bogolon ordering of p -wave types. As shown in Figs. 5(a) and 5(b), which are plots for Pomeranchuk instabilities ($\xi = D$), all the components, i.e., odd-parity multipoles and triplet and septet pair amplitudes, are regarded as order parameters since they are zero in Fig. 4 without symmetry breaking. Since the tendencies for $\eta = z$ and $\eta = x$ are similar, let us take a close look at the $\eta = z$ case in Fig. 5(a). The magnitudes of diagonal and off-diagonal components are nearly 70% and 30%, respectively. Namely, the major part of the contributions is from diagonal ones. Among them, the dominant one is the $\eta' = 1$ (monopole, or electron charge) component, which occupies 25%. Hence, although we consider the Pomeranchuk instability of bogolons, the dominant contribution is the same as that of electrons with a monopole where internal degrees of freedom are not reflected. Note that the other components also give contributions to the susceptibility, although they are smaller than the monopole contribution.

Actually, the dominant component from $(\xi', \eta') = (\bar{D}, 1)$ can be evaluated analytically since the multipole matrix $\check{O}^{\xi'=\bar{D}, \eta'=1}$ is proportional to the identity matrix. Then the expression for the susceptibility is substantially simplified, and we obtain

$$\chi_{\xi\eta}^{\bar{D},1} = \frac{\text{Tr} \check{n}_{\xi\eta} \text{Tr} \check{n}_{\xi\eta}^\dagger}{\text{Tr} [\check{n}_{\xi\eta} \check{n}_{\xi\eta}^\dagger] \text{Tr} \mathbb{1}} \chi_{\xi\eta}. \quad (40)$$

Hence, the value of 25% in Figs. 5(a) and 5(b) is the exact figure. This expression also explains the disappearance of the

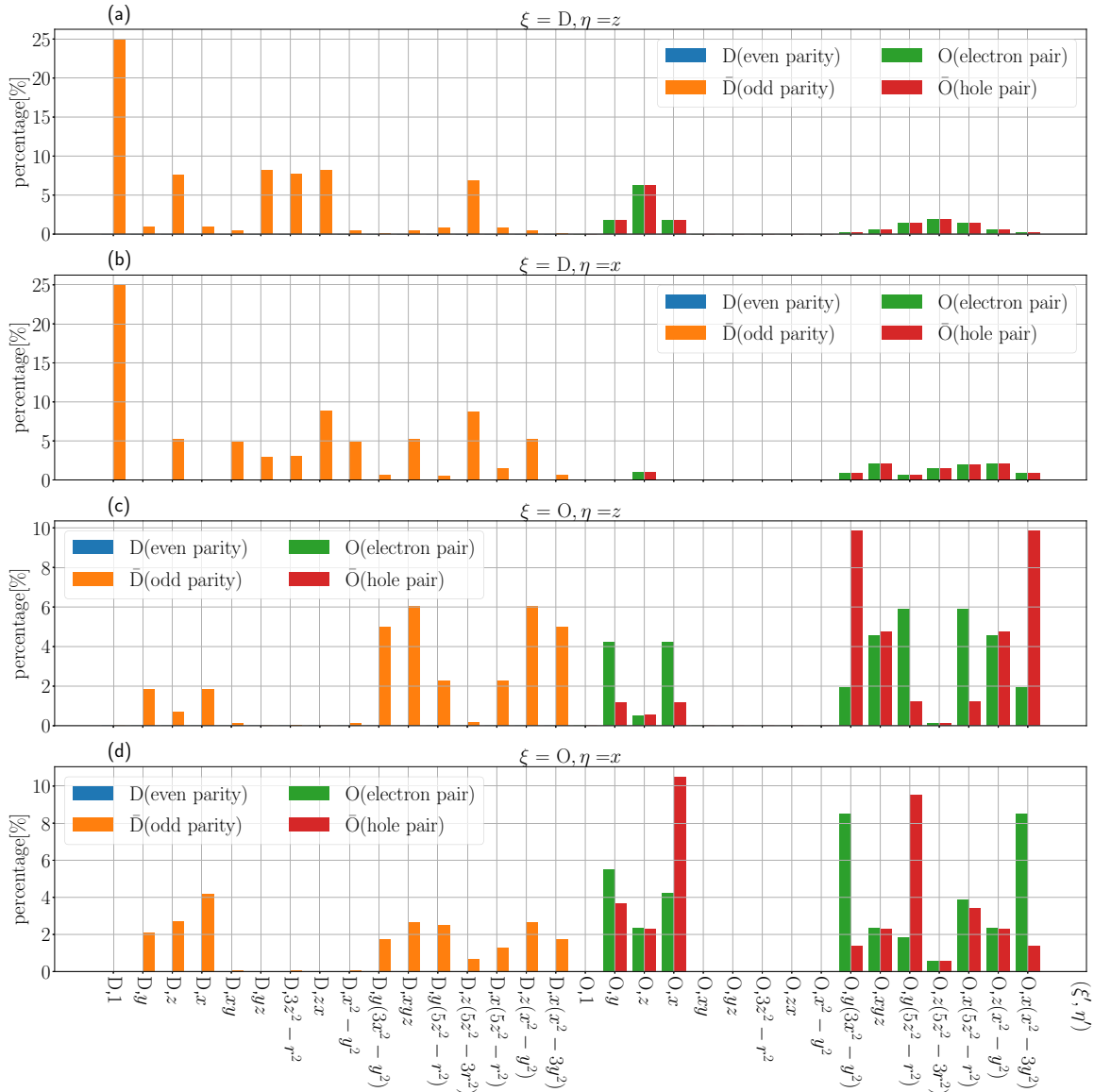


FIG. 5. Electron multipole components induced by p -wave (a,b) Pomeranchuk ($\xi = D$) and (c,d) Cooper ($\xi = O$) instabilities of bogolons with the form factors (a,c) $g_{\eta=z}(\mathbf{k}) \propto k_z$ and (b,d) $g_{\eta=x}(\mathbf{k}) \propto k_x$. The parameters are chosen to be $\beta/\varepsilon_F = 0.1$, $\Delta_0/\varepsilon_F = 0.1$, $\Delta_1/\varepsilon_F = 0.5$.

electron monopole contribution for the off-diagonal bogolon ordering discussed next since the matrix $\check{n}_{O,\eta}$ is traceless.

In Figs. 5(c) and 5(d) we show the susceptibility tensor for the order parameters of electrons induced by Cooper instability of bogolons ($\eta = z, x$). Since we expand the bogolon pair amplitude $\alpha_k^\dagger \alpha_{-k}^\dagger$, which is a non-Hermitian operator, the induced electron and hole pairs ($\xi' = O, \bar{O}$) have different magnitudes, in contrast to Figs. 5(a) and 5(b). In the case of $\eta = z$ in Fig. 5(c), the magnitudes for diagonal and off-diagonal components are nearly 30% and 70%, respectively, and the main contributions come from off-diagonal ones. The dominant contributions are the septet pairing with types $\eta' = y(3x^2 - y^2), x(x^2 - 3y^2)$ (each value is $\simeq 10\%$). However, these components are not as remarkable as the monopole in Figs. 5(a) and 5(b), and many pair amplitudes are induced simultaneously with comparable magnitudes. The basic trends for the $\eta = x$ case in Fig. 5(d) are similar to the $\eta = z$ case,

but the maximum contribution is the spin-triplet pair of $\eta' = x$ type. Hence, we conclude that the bogolons' Cooper pairs are dominantly contributed by the electron and hole pairs, while the main contribution of pair amplitudes is dependent on the types of bogolon order parameters. We note that the diagonal order parameters (electron multipoles) also give non-negligible contributions to bogolon Cooper pairs. Similar features are seen also in f -wave pairs of bogolons.

In this way the bogolon orderings partially inherit the properties of original electrons. However, the bogolons' order parameter cannot be simply identified as one dominant component of the electrons' order parameter. Hence, if one encounters the second phase transition inside the superconducting state, one cannot simply determine diagonal or off-diagonal order of the original electrons, and we should consider the possibility of bogolon orders, where the electron diagonal and off-diagonal order components are substantially

mixed with each other. In relation to this point, the possible relevance to real materials is discussed in the next section.

IV. SUMMARY AND DISCUSSION

In this paper we have theoretically studied the possibility of the Pomeranchuk and Cooper instabilities of Bogoliubov Fermi surfaces below the superconducting transition temperature. Using the $j = 3/2$ electron model with symmetric spin-orbit interaction plus time-reversal symmetry-broken even-parity pair potentials, we studied the physics arising from the remaining bogolon degrees of freedom at low temperatures in the weak-interaction limit. Based on the linear response theory, the bogolons' order parameters are systematically classified by using the multipole expansion for both diagonal and off-diagonal physical quantities of the original electrons, i.e., multipoles and multiplet pairs. These are also interpreted in the context of Landau free energy.

We numerically calculated the multipole expansion coefficients for the bogolons' order parameters. For Pomeranchuk instability of bogolons, the main contribution comes from the monopole of electrons, and hence, the Pomeranchuk instability of electron charge mainly occurs. For Cooper instability of bogolons, the main contribution is the pair amplitudes of the original electrons. Thus, the characters of electrons are partially inherited by bogolons. We emphasize that the other minor components also give a non-negligible contribution to bogolon's order parameters. Hence, below the superconducting transition temperature, there is no clear-cut answer for determining multipoles (diagonal) or multiplets (off-diagonal) as an order parameter for the second phase transition. Although we have used the concrete model of $j = 3/2$ electrons, our analysis relies on the presence of the Bogoliubov Fermi surfaces and can be applied to a wider class of materials. As a future perspective, while we have assumed the weak-coupling limit and the realization of one specific bogolon's ordering, it is an interesting problem to consider the concrete interaction in terms of the original electrons and to study the resultant ordering state of bogolons.

The bogolon orderings discussed in this paper could be a possible scenario for materials which possess a phase transition inside the superconducting phase. In $U_{1-x}Th_xBe_{13}$ [41–44], two successive superconducting transitions have been observed. The first transition at higher temperature can be identified as the superconducting order parameter, but the origin and the order parameter for the second transition have been argued. The candidates are magnetic ordering and the second superconducting order parameter with time-reversal symmetry breaking [43,44]. In light of the present paper, we propose that the second transition cannot be simply classified into either diagonal (e.g., magnetic order) or off-diagonal (i.e., pairing state) orders in a strict sense, but rather, they are mixed with each other in the presence of spin-orbital coupling.

On the other hand, in $U_{1-x}Th_xBe_{13}$ when applying pressure, whereas the second transition is not observed, the finite specific heat coefficient is found at temperatures much lower than the transition point [45]. The remaining specific heat coefficient is also observed in the recently found superconductor UTe_2 [46,47], and the remaining Fermi surface is suspected to be one of the possible origins [48]. Hence, one expects

some second orderings utilizing the degrees of freedom from Fermi surfaces at further low temperatures or by tuning the system. Indeed, the various superconducting phases with multiple phase transitions were recently identified in UTe_2 under pressure and magnetic field [49,50]. Although ordinary superconductors do not have degrees of freedom below the transition temperature, the existence of the second phase transition indicates the presence of the remaining degrees of freedom, which could be the existing Bogoliubov Fermi surfaces.

For another class of superconducting materials, recently, the rotational symmetry breaking was found in Bi_2Se_3 - and iron-based materials [51–55] only in the superconducting state, which is called nematic superconductivity [56]. It was proposed in Ref. [57] that the superconducting state itself can produce the rotational symmetry breaking. On the other hand, if the second transition is identified as it is separated from the first superconducting transition, there could be the possibility of ordering instability of the remaining Fermi surface degrees of freedom. Thus, the insights in this paper will be useful for identifying the mechanisms and for analyzing the properties of superconductors which have second phase transitions.

ACKNOWLEDGMENTS

This work was supported by JSPS KAKENHI Grants No. JP18K13490, No. JP18H01176, No. JP18H04305, and No. JP19H01842.

APPENDIX A: MULTIPOLE AND MULTIPLLET PAIR OPERATORS

1. Multipoles

We consider the electronic multipole operator in Eq. (9), which is composed of

$$M^{\prime}(\mathbf{k}) = \tilde{c}_k^{\dagger} \hat{O}^{\prime} \tilde{c}_k. \quad (A1)$$

The matrices are defined by

$$\hat{O}^1 = \sqrt{\frac{5}{4}} \hat{1} \quad (A2)$$

for the monopole (charge),

$$\hat{O}^y = \hat{J}_y = \frac{i}{2} \begin{pmatrix} 0 & -\sqrt{3} & & \\ \sqrt{3} & 0 & -2 & \\ & 2 & 0 & -\sqrt{3} \\ & & \sqrt{3} & 0 \end{pmatrix}, \quad (A3)$$

$$\hat{O}^z = \hat{J}_z = \frac{1}{2} \begin{pmatrix} 3 & & & \\ & 1 & & \\ & & -1 & \\ & & & -3 \end{pmatrix}, \quad (A4)$$

$$\hat{O}^x = \hat{J}_x = \frac{1}{2} \begin{pmatrix} 0 & \sqrt{3} & & \\ \sqrt{3} & 0 & 2 & \\ & 2 & 0 & \sqrt{3} \\ & & \sqrt{3} & 0 \end{pmatrix} \quad (A5)$$

for the dipole,

$$\hat{O}^{xy} = \sqrt{\frac{5}{3}} [\hat{J}_x \hat{J}_y], \quad (\text{A6})$$

$$\hat{O}^{yz} = \sqrt{\frac{5}{3}} [\hat{J}_y \hat{J}_z], \quad (\text{A7})$$

$$\hat{O}^{3z^2-r^2} = \sqrt{\frac{5}{36}} (3\hat{J}_z^2 - \hat{J}^2), \quad (\text{A8})$$

$$\hat{O}^{zx} = \sqrt{\frac{5}{3}} [\hat{J}_z \hat{J}_x], \quad (\text{A9})$$

$$\hat{O}^{x^2-y^2} = \sqrt{\frac{5}{12}} (\hat{J}_x^2 - \hat{J}_y^2) \quad (\text{A10})$$

for the quadrupole, and

$$\hat{O}^{y(3x^2-y^2)} = \sqrt{\frac{5}{18}} [\hat{J}_y (3\hat{J}_x^2 - \hat{J}_y^2)], \quad (\text{A11})$$

$$\hat{O}^{xyz} = \sqrt{\frac{20}{3}} [\hat{J}_x \hat{J}_y \hat{J}_z], \quad (\text{A12})$$

$$\hat{O}^{y(5z^2-r^2)} = \sqrt{\frac{5}{30}} [\hat{J}_y (5\hat{J}_z^2 - \hat{J}^2)], \quad (\text{A13})$$

$$\hat{O}^{z(5z^2-3r^2)} = \sqrt{\frac{5}{45}} \hat{J}_z (5\hat{J}_z^2 - 3\hat{J}^2), \quad (\text{A14})$$

$$\hat{O}^{x(5z^2-r^2)} = \sqrt{\frac{5}{30}} [\hat{J}_x (5\hat{J}_z^2 - \hat{J}^2)], \quad (\text{A15})$$

$$\hat{O}^{z(x^2-y^2)} = \sqrt{\frac{5}{3}} [\hat{J}_z (\hat{J}_x^2 - \hat{J}_y^2)], \quad (\text{A16})$$

$$\hat{O}^{x(x^2-3y^2)} = \sqrt{\frac{5}{18}} [\hat{J}_x (\hat{J}_x^2 - 3\hat{J}_y^2)] \quad (\text{A17})$$

for the octupole, where the square brackets $[\dots]$ make the operators symmetric and Hermitian as $[ABC] = (ABC + ACB + BCA + BAC + CAB + CBA)/3!$, for example. The above matrices are normalized as $\text{Tr}[(\hat{O}^{\eta'})^2] = 5$.

2. Multiplet pairs

We also define the antisymmetric tensor

$$\hat{E} = \begin{pmatrix} & & & 1 \\ & & -1 & \\ & 1 & & \\ -1 & & & \end{pmatrix}, \quad (\text{A18})$$

with which the pairing amplitude for electrons is defined as

$$P^{\eta'}(\mathbf{k}) = \bar{c}_k^\dagger \hat{O}^{\eta'} \hat{E} \bar{c}_{-\mathbf{k}}^{\dagger\text{T}}. \quad (\text{A19})$$

Here the meaning of $\hat{O}^{\eta'} \hat{E}$ can be intuitively understood by comparing it with the two-body wave function composed of $j = 3/2$ spins. Let us consider the two-body wave function $|JM\rangle$ ($M \in [-J, J]$) composed of two $j = 3/2$ spins with the single-body wave function $|m\rangle$ ($m \in [-j, j]$), which mimics the Cooper pair made of two electrons. The wave function is classified by the total spins $J = 0, 1, 2, 3$, which correspond to the spin-singlet, spin-triplet, spin-quintet, and spin-septet states. More specifically, we define the two-body

wave function

$$|\eta'\rangle = \sum_{mm'} (\hat{O}^{\eta'} \hat{E})_{mm'} |m\rangle_1 |m'\rangle_2, \quad (\text{A20})$$

and the full correspondence between the two-body states $|\eta'\rangle$ and $|JM\rangle$ is given as

$$|\eta' = 1\rangle \propto |0, 0\rangle \quad (\text{A21})$$

for the spin-singlet state,

$$|\eta' = y\rangle \propto |1, 1\rangle + |1, -1\rangle, \quad (\text{A22})$$

$$|\eta' = z\rangle \propto |1, 0\rangle, \quad (\text{A23})$$

$$|\eta' = x\rangle \propto |1, 1\rangle - |1, -1\rangle \quad (\text{A24})$$

for the spin-triplet states,

$$|\eta' = xy\rangle \propto |2, 2\rangle - |2, -2\rangle, \quad (\text{A25})$$

$$|\eta' = yz\rangle \propto |2, 1\rangle + |2, -1\rangle, \quad (\text{A26})$$

$$|\eta' = 3z^2 - r^2\rangle \propto |2, 0\rangle, \quad (\text{A27})$$

$$|\eta' = zx\rangle \propto |2, 1\rangle - |2, -1\rangle, \quad (\text{A28})$$

$$|\eta' = x^2 - y^2\rangle \propto |2, 2\rangle + |2, -2\rangle \quad (\text{A29})$$

for the spin-quintet states, and

$$|\eta' = y(3x^2 - y^2)\rangle \propto |3, 3\rangle + |3, -3\rangle, \quad (\text{A30})$$

$$|\eta' = xyz\rangle \propto |3, 2\rangle - |3, -2\rangle, \quad (\text{A31})$$

$$|\eta' = y(5z^2 - r^2)\rangle \propto |3, 1\rangle + |3, -1\rangle, \quad (\text{A32})$$

$$|\eta' = z(5z^2 - 3r^2)\rangle \propto |3, 0\rangle, \quad (\text{A33})$$

$$|\eta' = x(5z^2 - r^2)\rangle \propto |3, 1\rangle - |3, -1\rangle, \quad (\text{A34})$$

$$|\eta' = z(x^2 - y^2)\rangle \propto |3, 2\rangle + |3, -2\rangle, \quad (\text{A35})$$

$$|\eta' = x(x^2 - 3y^2)\rangle \propto |3, 3\rangle - |3, -3\rangle \quad (\text{A36})$$

for the spin-septet states. These relations are checked by the construction using Clebsch-Gordan coefficients. Obviously, we can see the analogy to the s, p, d, f electrons' wave functions of the hydrogen atom written by polynomials of spatial coordinates. For the electron pair amplitudes, we only have to replace $|m\rangle_1$ by c_{km}^\dagger and $|m'\rangle_2$ by $c_{-k,m'}^\dagger$.

3. Orthonormality

With the above matrices, we define the 8×8 matrices by

$$\check{O}^{\text{D}\eta'} = \sqrt{\frac{1}{10}} \begin{pmatrix} \hat{O}^{\eta'} & \hat{0} \\ \hat{0} & -\hat{O}^{\eta'\text{T}} \end{pmatrix}, \quad (\text{A37})$$

$$\check{O}^{\text{D}\bar{\eta}'} = \sqrt{\frac{1}{10}} \begin{pmatrix} \hat{O}^{\eta'} & \hat{0} \\ \hat{0} & \hat{O}^{\eta'\text{T}} \end{pmatrix}, \quad (\text{A38})$$

$$\check{O}^{\text{O}\eta'} = \sqrt{\frac{1}{5}} \begin{pmatrix} \hat{0} & \hat{O}^{\eta'} \hat{E} \\ \hat{0} & \hat{0} \end{pmatrix}, \quad (\text{A39})$$

$$\check{O}^{\text{O}\bar{\eta}'} = \sqrt{\frac{1}{5}} \begin{pmatrix} \hat{0} & \hat{0} \\ \hat{E}^\dagger \hat{O}^{\eta'\dagger} & \hat{0} \end{pmatrix}, \quad (\text{A40})$$

which correspond to even-parity ($\xi' = \text{D}$) and odd-parity ($\xi' = \bar{\text{D}}$) multipoles and electron-pair ($\xi' = \text{O}$) and hole-pair ($\xi' = \bar{\text{O}}$) amplitudes of the original electrons, respectively. Here the information for parity enters into the expression since the top left block of \check{O} originates from \vec{c}_k and the bottom right block originates from \vec{c}_{-k} . Note that further higher-order multipoles are not necessary. These matrices satisfy the orthonormal relation

$$\text{Tr}(\check{O}^{\xi_1 \eta_1 \dagger} \check{O}^{\xi_2 \eta_2}) = \delta_{\xi_1 \xi_2} \delta_{\eta_1 \eta_2}. \quad (\text{A41})$$

Then any 8×8 matrix \check{A} can be expanded as

$$\check{A} = \sum_{\xi' \eta'} a^{\xi' \eta'} \check{O}^{\xi' \eta'}, \quad (\text{A42})$$

and the expansion coefficients are extracted as

$$a^{\xi' \eta'} = \text{Tr}(\check{O}^{\xi' \eta' \dagger} \check{A}). \quad (\text{A43})$$

Hence, the series of above matrices (A37)–(A40) can be regarded as complete. With this property one can show the relation

$$\sum_{\xi' \eta'} \text{Tr}(\check{O}^{\xi' \eta' \dagger} \check{A}) \text{Tr}(\check{O}^{\xi' \eta'} \check{B}) = \text{Tr}(\check{A} \check{B}) \quad (\text{A44})$$

for arbitrary matrices \check{A} and \check{B} . This relation is useful in confirming the sum rule (15) in the main text.

APPENDIX B: k -DEPENDENT FORM FACTORS

In Eqs. (6) and (10), we consider the k -dependent form factor

$$g_\eta(\mathbf{k}) = g'_\eta(k, k_z) f_\eta(\phi), \quad (\text{B1})$$

with the cylindrical coordinate system $\mathbf{k} = (k, \phi, k_z)$. The complete functional forms are given by

$$g'_1 = \sqrt{\frac{1}{4\pi}}, \quad f_1 = 1 \quad (\text{B2})$$

for s waves,

$$g'_y = \sqrt{\frac{3}{4\pi}} \frac{k}{|\mathbf{k}|}, \quad f_y = \sin \phi, \quad (\text{B3})$$

$$g'_z = \sqrt{\frac{3}{4\pi}} \frac{k_z}{|\mathbf{k}|}, \quad f_z = 1, \quad (\text{B4})$$

$$g'_x = \sqrt{\frac{3}{4\pi}} \frac{k}{|\mathbf{k}|}, \quad f_x = \cos \phi \quad (\text{B5})$$

for p waves,

$$g'_{xy} = \sqrt{\frac{15}{16\pi}} \frac{k^2}{|\mathbf{k}|^2}, \quad f_{xy} = \sin 2\phi, \quad (\text{B6})$$

$$g'_{yz} = \sqrt{\frac{15}{4\pi}} \frac{k k_z}{|\mathbf{k}|^2}, \quad f_{yz} = \sin \phi, \quad (\text{B7})$$

$$g'_{3z^2-r^2} = \sqrt{\frac{5}{16\pi}} \frac{3k_z^2 - |\mathbf{k}|^2}{|\mathbf{k}|^2}, \quad f_{3z^2-r^2} = 1, \quad (\text{B8})$$

$$g'_{zx} = \sqrt{\frac{15}{4\pi}} \frac{k k_z}{|\mathbf{k}|^2}, \quad f_{zx} = \cos \phi, \quad (\text{B9})$$

$$g'_{x^2-y^2} = \sqrt{\frac{15}{16\pi}} \frac{k^2}{|\mathbf{k}|^2}, \quad f_{x^2-y^2} = \cos 2\phi \quad (\text{B10})$$

for d waves, and

$$g'_{y(3x^2-y^2)} = \sqrt{\frac{35}{32\pi}} \frac{k^3}{|\mathbf{k}|^3}, \quad f_{y(3x^2-y^2)} = \sin 3\phi, \quad (\text{B11})$$

$$g'_{xyz} = \sqrt{\frac{105}{16\pi}} \frac{k^2 k_z}{|\mathbf{k}|^3}, \quad f_{xyz} = \sin 2\phi, \quad (\text{B12})$$

$$g'_{y(5z^2-r^2)} = \sqrt{\frac{21}{32\pi}} \frac{k(5k_z^2 - |\mathbf{k}|^2)}{|\mathbf{k}|^3}, \quad f_{y(5z^2-r^2)} = \sin \phi, \quad (\text{B13})$$

$$g'_{z(5z^2-3r^2)} = \sqrt{\frac{7}{16\pi}} \frac{k_z(5k_z^2 - 3|\mathbf{k}|^2)}{|\mathbf{k}|^3}, \quad f_{z(5z^2-3r^2)} = 1, \quad (\text{B14})$$

$$g'_{x(5z^2-r^2)} = \sqrt{\frac{21}{32\pi}} \frac{k(5k_z^2 - |\mathbf{k}|^2)}{|\mathbf{k}|^3}, \quad f_{x(5z^2-r^2)} = \cos \phi, \quad (\text{B15})$$

$$g'_{z(x^2-y^2)} = \sqrt{\frac{105}{16\pi}} \frac{k^2 k_z}{|\mathbf{k}|^3}, \quad f_{z(x^2-y^2)} = \cos 2\phi, \quad (\text{B16})$$

$$g'_{x(x^2-3y^2)} = \sqrt{\frac{35}{32\pi}} \frac{k^3}{|\mathbf{k}|^3}, \quad f_{x(x^2-3y^2)} = \cos 3\phi \quad (\text{B17})$$

for f waves, where $|\mathbf{k}| = \sqrt{k^2 + k_z^2}$. The coefficients are determined by the normalization condition

$$\int d\Omega_{\mathbf{k}} |g_\eta(\mathbf{k})|^2 = 1, \quad (\text{B18})$$

where $\int d\Omega_{\mathbf{k}}$ means the integral over the spherical surface. Note that one can consider further higher-order functions since there is an infinite number of degrees of freedom in \mathbf{k} space. If one uses the Fourier expansion by utilizing the function $f_\eta(\phi)$, one can, in principle, decompose $\chi_{\xi\eta}^{\xi'\eta'}$ further depending on the rotational symmetry breaking in the xy plane.

- [1] I. I. Pomeranchuk, J. Exp. Theor. Phys. **35**, 524 (1958).
 [2] J. Kondo, Prog. Theor. Phys. **32**, 37 (1964).
 [3] K. Yosida, Phys. Rev. **147**, 223 (1966).
 [4] L. N. Cooper, Phys. Rev. **104**, 1189 (1956).

- [5] J. Bardeen, L. N. Cooper, and J. R. Schrieffer, Phys. Rev. **108**, 1175 (1957).
 [6] N. N. Bogoliubov, Sov. Phys. JETP **34**, 41 (1958).
 [7] G. E. Volovik, Phys. Lett. A **142**, 282 (1989).

- [8] W. V. Liu and F. Wilczek, *Phys. Rev. Lett.* **90**, 047002 (2003).
- [9] E. Gubankova, E. G. Mishchenko, and F. Wilczek, *Phys. Rev. Lett.* **94**, 110402 (2005); *Phys. Rev. B* **74**, 184516 (2006).
- [10] D. F. Agterberg, P. M. R. Brydon, and C. Timm, *Phys. Rev. Lett.* **118**, 127001 (2017).
- [11] P. M. R. Brydon, D. F. Agterberg, H. Menke, and C. Timm, *Phys. Rev. B* **98**, 224509 (2018).
- [12] N. F. Q. Yuan and L. Fu, *Phys. Rev. B* **97**, 115139 (2018).
- [13] S. Sumita, T. Nomoto, K. Shiozaki, and Y. Yanase, *Phys. Rev. B* **99**, 134513 (2019).
- [14] J. M. Link, I. Boettcher, and I. F. Herbut, *Phys. Rev. B* **101**, 184503 (2020).
- [15] G. E. Volovik, *JETP Lett.* **58**, 469 (1993).
- [16] K. A. Moler, D. J. Baar, J. S. Urbach, R. Liang, W. N. Hardy, and A. Kapitulnik, *Phys. Rev. Lett.* **73**, 2744 (1994).
- [17] S. Autti, J. T. Mäkinen, J. Rysti, G. E. Volovik, V. V. Zavjalov, and V. B. Eltsov, [arXiv:2002.11492](https://arxiv.org/abs/2002.11492).
- [18] H. Oh and E.-G. Moon, [arXiv:1911.08487](https://arxiv.org/abs/1911.08487).
- [19] P. M. R. Brydon, L. Wang, M. Weinert, and D. F. Agterberg, *Phys. Rev. Lett.* **116**, 177001 (2016).
- [20] H. Menke, C. Timm, and P. M. R. Brydon, *Phys. Rev. B* **100**, 224505 (2019).
- [21] S. Kobayashi, A. Yamakage, Y. Tanaka, and M. Sato, *Phys. Rev. Lett.* **123**, 097002 (2019).
- [22] K. I. Kugel and D. I. Khomskii, *Sov. Phys. JETP Lett.* **15**, 446 (1972).
- [23] F. J. Ohkawa, *J. Phys. Soc. Jpn.* **52**, 3897 (1983).
- [24] R. Shiina, H. Shiba, and P. Thalmeier, *J. Phys. Soc. Jpn.* **66**, 1741 (1997).
- [25] Y. Kuramoto and H. Kusunose, *J. Phys. Soc. Jpn.* **69**, 671 (2000).
- [26] P. Santini and G. Amoretti, *Phys. Rev. Lett.* **85**, 2188 (2000).
- [27] T. Takimoto, *J. Phys. Soc. Jpn.* **75**, 034714 (2005).
- [28] H. Kusunose, *J. Phys. Soc. Jpn.* **77**, 064710 (2008).
- [29] For a review, see Y. Kuramoto, H. Kusunose, and A. Kiss, *J. Phys. Soc. Jpn.* **78**, 072001 (2009).
- [30] K. Haule and G. Kotliar, *Nat. Phys.* **5**, 796 (2009).
- [31] H. Ikeda, M.-T. Suzuki, R. Arita, T. Takimoto, T. Shibauchi, and Y. Matsuda, *Nat. Phys.* **8**, 528 (2012).
- [32] M.-T. Suzuki, T. Koretsune, M. Ochi, and R. Arita, *Phys. Rev. B* **95**, 094406 (2017).
- [33] S. Hayami, M. Yatsushiro, Y. Yanagi, and H. Kusunose, *Phys. Rev. B* **98**, 165110 (2018).
- [34] For reviews, see Y. Tanaka, M. Sato, and N. Nagaosa, *J. Phys. Soc. Jpn.* **81**, 011013 (2012); J. Linder and A. V. Balatsky, *Rev. Mod. Phys.* **91**, 045005 (2019).
- [35] S. Hoshino, P. Werner, and R. Arita, *Phys. Rev. B* **99**, 235133 (2019).
- [36] P. Coleman, E. Miranda, and A. Tsvelik, *Phys. Rev. Lett.* **70**, 2960 (1993).
- [37] P. Coleman, E. Miranda, and A. Tsvelik, *Phys. Rev. B* **49**, 8955 (1994).
- [38] S. Hoshino and Y. Kuramoto, *Phys. Rev. Lett.* **112**, 167204 (2014).
- [39] S. Hoshino, *Phys. Rev. B* **90**, 115154 (2014).
- [40] S. Hoshino, K. Yada, and Y. Tanaka, *Phys. Rev. B* **93**, 224511 (2016).
- [41] J. L. Smith, Z. Fisk, J. O. Willis, A. L. Giorgi, R. B. Roof, H. R. Ott, H. Rudigier, and E. Felder, *Phys. B (Amsterdam, Neth.)* **135**, 3 (1985).
- [42] H. R. Ott, H. Rudigier, Z. Fisk, and J. L. Smith, *Phys. Rev. B* **31**, 1651(R) (1985).
- [43] R. H. Heffner, J. L. Smith, J. O. Willis, P. Birrer, C. Baines, F. N. Gygax, B. Hitti, E. Lippelt, H. R. Ott, A. Schenck, E. A. Knetsch, J. A. Mydosh, and D. E. McLaughlin, *Phys. Rev. Lett.* **65**, 2816 (1990).
- [44] Y. Shimizu, S. Kittaka, S. Nakamura, T. Sakakibara, D. Aoki, Y. Homma, A. Nakamura, and K. Machida, *Phys. Rev. B* **96**, 100505(R) (2017).
- [45] R. J. Zieve, R. Duke, and J. L. Smith, *Phys. Rev. B* **69**, 144503 (2004).
- [46] S. Ran, C. Eckberg, Q.-P. Ding, Y. Furukawa, T. Metz, S. R. Saha, I.-L. Liu, M. Zic, H. Kim, J. Paglione, and N. P. Butch, *Science* **365**, 684 (2019).
- [47] D. Aoki, A. Nakamura, F. Honda, D. Li, Y. Homma, Y. Shimizu, Y. J. Sato, G. Knebel, J.-P. Brison, A. Pourret, D. Braithwaite, G. Lapertot, Q. Niu, M. Vališka, H. Harima, and J. Flouquet, *J. Phys. Soc. Jpn.* **88**, 043702 (2019).
- [48] T. Metz, S. Bae, S. Ran, I.-L. Liu, Y. S. Eo, W. T. Fuhrman, D. F. Agterberg, S. M. Anlage, N. P. Butch, and J. Paglione, *Phys. Rev. B* **100**, 220504(R) (2019).
- [49] I. M. Hayes, D. S. Wei, T. Metz, J. Zhang, Y. S. Eo, S. Ran, S. R. Saha, J. Collini, N. P. Butch, D. F. Agterberg, A. Kapitulnik, and J. Paglione, [arXiv:2002.02539](https://arxiv.org/abs/2002.02539).
- [50] D. Aoki, F. Honda, G. Knebel, D. Braithwaite, A. Nakamura, D. Li, Y. Homma, Y. Shimizu, Y. J. Sato, J.-P. Brison, and J. Flouquet, *J. Phys. Soc. Jpn.* **89**, 053705 (2020).
- [51] K. Matano, M. Kriener, K. Segawa, Y. Ando, and G.-Q. Zheng, *Nat. Phys.* **12**, 852 (2016).
- [52] S. Yonezawa, K. Tajiri, S. Nakata, Y. Nagai, Z. Wang, K. Segawa, Y. Ando, and Y. Maeno, *Nat. Phys.* **13**, 123 (2017).
- [53] Y. Pan, A. M. Nikitin, G. K. Araizi, Y. K. Huang, Y. Matsushita, T. Naka, and A. de Visser, *Sci. Rep.* **6**, 28632 (2016).
- [54] T. Asaba, B. J. Lawson, C. Tinsman, L. Chen, P. Corbae, G. Li, Y. Qiu, Y. S. Hor, L. Fu, and L. Li, *Phys. Rev. X* **7**, 011009 (2017).
- [55] Y. S. Kushnirenko, D. V. Evtushinsky, T. K. Kim, I. V. Morozov, L. Harnagea, S. Wurmehl, S. Aswartham, A. V. Chubukov, and S. V. Borisenko, [arXiv:1810.04446](https://arxiv.org/abs/1810.04446).
- [56] For a review, see S. Yonezawa, *Condens. Matter* **4**, 2 (2019).
- [57] L. Fu, *Phys. Rev. B* **90**, 100509(R) (2014).